(19) Europäisches Patentamt
European Patent Office
Office européen des brevets

(11) **EP 1 737 055 B1**

(12) **EUROPEAN PATENT SPECIFICATION**

(45) Date of publication and mention of the grant of the patent:
**11.01.2012 Bulletin 2012/02**

(21) Application number: **05720955.3**

(22) Date of filing: **10.03.2005**

(51) Int Cl.:
***H01L 43/08*** *(2006.01)* ***H01L 43/10*** *(2006.01)*
***H01L 43/12*** *(2006.01)* ***H01F 10/32*** *(2006.01)*

(86) International application number:
**PCT/JP2005/004720**

(87) International publication number:
**WO 2005/088745 (22.09.2005 Gazette 2005/38)**

# (54) MAGNETORESISTIVE ELEMENT AND ITS MANUFACTURING METHOD

MAGNETWIDERSTANDSELEMENT UND VERFAHREN ZU SEINER HERSTELLUNG

ÉLÉMENT MAGNÉTORÉSISTIF ET SA MÉTHODE DE PRODUCTION

(84) Designated Contracting States:
**DE FR**

(30) Priority: **12.03.2004 JP 2004071186**
**28.10.2004 JP 2004313350**

(43) Date of publication of application:
**27.12.2006 Bulletin 2006/52**

(73) Proprietor: **Japan Science and Technology Agency**
**Kawaguchi-shi,**
**Saitama 332-0012 (JP)**

(72) Inventor: **YUASA, Shinji,**
**c/o Tsukuba Central 2**
**Tsukuba-shi,**
**Ibaraki 3058568 (JP)**

(74) Representative: **Hengelhaupt, Jürgen et al**
**Gulde Hengelhaupt Ziebig & Schneider**
**Patentanwälte - Rechtsanwälte**
**Wallstrasse 58/59**
**10179 Berlin (DE)**

(56) References cited:
**EP-A- 1 633 007** **EP-A2- 1 085 586**
**JP-A- 2002 204 004** **JP-A- 2002 289 943**
**JP-A- 2003 204 010** **JP-A- 2003 318 465**

- **MITANI S ET AL: "Fe/MgO/FeCo(100) epitaxial magnetic tunnel junctions prepared by using in situ plasma oxidation" JOURNAL OF APPLIED PHYSICS, vol. 93, no. 10, 15 May 2003 (2003-05-15), pages 8041-8043, XP012058375 ISSN: 0021-8979**
- **BOWEN M ET AL: "Large magnetoresistance in Fe/MgO/FeCo(001) epitaxial tunnel junctions on GaAs(001)" APPLIED PHYSICS LETTERS, vol. 79, no. 11, 10 September 2001 (2001-09-10), pages 1655-1657, XP012028861 ISSN: 0003-6951**
- **POPOVA E ET AL: "Epitaxial MgO layer for low-resistance and coupling-free magnetic tunnel junctions" APPLIED PHYSICS LETTERS, vol. 81, no. 6, 5 August 2002 (2002-08-05), pages 1035-1037, XP012033155 ISSN: 0003-6951**
- **MARTINEZ BOUBETA C ET AL: "Magnetic coupling in epitaxial TM/MgO/Fe(001) (TM=FeCo, Fe/Co, Fe) macroscopic and microscopic trilayers" JOURNAL OF APPLIED PHYSICS, vol. 94, no. 6, 15 September 2003 (2003-09-15), pages 4006-4012, XP012060211 ISSN: 0021-8979**



EP 1 737 055 B1

## Description

### BACKGROUND OF THE INVENTION

#### Field of the Invention

**[0001]** The present invention relates to a magnetic tunnel junction device and a method of manufacturing the same, particularly to a magnetic tunnel junction device with a high magnetoresistance and a method of manufacturing the same.

#### Description of Related Art

**[0002]** Magnetoresistive random access memories (MRAMs) refer to a large-scale integrated memory circuit that is expected to replace the currently widely used DRAM memories. Research and development of MRAM devices, which are fast and non-volatile memory devices, are being extensively carried out, and sample products of a 4Mbit MRAM have actually been delivered.

**[0003]** Fig. 8 shows the structure and operation principle of a magnetic tunnel junction device (to be hereafter referred to as a "MTJ device"), which is the most important part of the MRAM. As shown in Fig. 8(A), a MTJ device comprises a tunnelling junction structure in which a tunnel barrier (to be hereafter also referred to as a "barrier layer") made of an oxide is sandwiched between a first and a second electrode made of a ferromagnetic metal. The tunnel barrier layer comprises an amorphous Al-O layer (see Non-Patent Document 1). As shown in Fig. 8(A), in the case of parallel magnetization alignment where the directions of magnetizations of the first and second ferromagnetic electrodes are aligned parallel, the electric resistance of the device with respect to the direction normal to the interfaces of the tunneling junction structure decreases. On the other hand, in the case of antiparallel magnetization alignment where the directions of magnetizations of the first and second ferromagnetic electrodes are aligned antiparallel as shown in Fig. 8(B), the electric resistance with respect to the direction normal to the interfaces of the tunneling junction structure increases. The resistance value does not change in a general state, so that information "1" or "0" can be stored depending on whether the resistance value is high or not. Since the parallel and antiparallel magnetization alignments can be stored in a non-volatile fashion, the device can be used as a non-volatile memory device.

**[0004]** Fig. 9 shows an example of the basic structure of the MRAM. Fig. 9(A) shows a perspective view of the MRAM, and Fig. 9(B) schematically shows a circuit block diagram Fig. 9(C) is a cross-section of an example of the structure of the MRAM. Referring to Fig. 9(A), in an MRAM, a word line WL and a bit line BL are disposed in an intersecting manner, with an MRAM cell disposed at each intersection. As shown in Fig. 9(B), the MRAM cell disposed at the intersection of a word line and a bit line comprises a MTJ device and a MOSFET directly connected to the MTJ device. Stored information can be read by reading the resistance value of the MTJ device that functions as a load resistance, using the MOSFET. The stored information can be rewritten by applying a magnetic field to the MTJ device, for example. As shown in Fig. 9(C), an MRAM memory cell comprises a MOSFET 100 including a source region 103 and a drain region 105 both formed inside a p-type Si substrate 101, and a gate electrode 111 formed on a channel region that is defined between the source and drain regions. The MRAM also comprises a MTJ device 117. The source region 103 is grounded, and the drain is connected to a bit line BL via the MTJ device. A word line WL is connected to the gate electrode 111 in a region that is not shown.

**[0005]** Thus, a single non-volatile MRAM memory cell can be formed by a single MOSFET 100 and a single MTJ device 117. The MRAMs are therefore suitable where high levels of integration are required.

Non-Patent Document 1: D. Wang, et al.: Science 294 (2001) 1488.
Non-Patent Document 2: S. Mitani et al: Journal of Applied Physics 93 (2003) 8041-8043

### SUMMARY OF THE INVENTION

**[0006]** Although there are prospects for achieving MRAMs with capacities on the order of 64Mbits based on the current technologies, the characteristics of the MTJ device, which is the heart of MRAM, needs to be improved if higher levels of integration are to be achieved. In particular, in order to increase the output voltage of the MTJ device, the magnetoresistance must be increased and the bias voltage characteristics must be improved. Fig. 10 illustrates how the magnetoresistance in a conventional MTJ device using an amorphous Al-O as the tunnel barrier changes as a function of the bias voltage (L1). As shown, in the conventional MTJ device, the magnetoresistance is small and, notably, it tends to drastically decrease upon application of bias voltage. With such characteristics, the output voltage when operation margins are taken into consideration is too small for the device to be employed for an actual memory device. Specifically, the magnetoresistance of the current MTJ device is small at approximately 70%, and the output voltage is also small at no more than 200 mV, which is substantially half the output voltage of a DRAM. This has resulted in the problem that

as the level of integration increases, signals are increasingly lost in noise and cannot be read.

**[0007]** Fully epitaxial (001) FeCo/MgO/Fe MTJ devices have been realised in Document 2, for example. Barrier heights are typically 0.9 cV.

**[0008]** It is an object of the invention to increase the output voltage of a MTJ device. It is another object of the invention to provide a memory device with a high magnetoresistance for stable operation.

**[0009]** In one aspect, the invention provides a magnetoresistive device comprising a magnetic tunnel junction structure comprising: a tunnel barrier layer; a first ferromagnetic material layer of an Fe alloy in the BCC structure formed on a first side of the tunnel barrier layer; and a second ferromagnetic material layer of an Fe alloy in the BCC structure formed on a second side of the tunnel barrier layer, wherein the tunnel barrier layer is formed by a poly-crystalline $MgO_x$ layer, wherein $0 < x < 1$, in which the (001) crystal plane is preferentially oriented, and a potential barrier in the range of 0.2 to 0.5 eV, as set out in claim 1.

**[0010]** In other aspects, the invention provides a tunnel barrier as set out in claim 3 and a method of manufacturing as set out in claim 4.

## BRIEF DESCRIPTION OF THE DRAWINGS

**[0011]**

Fig. 1(B) shows the structure of a MTJ device according to a first embodiment of the invention, and Fig. 1(A) shows the energy band structure of a ferromagnetic metal Fe(001), illustrating the $E\text{-}E_F$ relationship with respect to the [001] direction of the momentum space.

Fig. 2(A) to Fig. 2(D) schematically show the process of manufacturing a MTJ device with a Fe(001)/MgO(001)/Fe (001) structure (to be hereafter referred to as a "Fe(001)/MgO(001)/Fe(001) MTJ device").

Fig. 3(A) shows a RHEED image of a Fe(001) lower electrode (a first electrode), and Fig. 3(B) shows a RHEED image of a MgO(001) barrier layer.

Fig. 4 shows the results of observing the quadrupole mass spectra in the deposition chamber during the MgO evaporation.

Fig. 5 shows the film deposition rate dependency of the oxygen partial pressure during the MgO evaporation.

Fig. 6 shows typical magnetoresistance curves of the Fe(001)/MgO(001)/Fe(001) MTJ device.

Fig. 7(A) shows the bias voltage dependency of the MR ratio at room temperature, and Fig. 7(B) shows the output voltage $V_{out}$ of the MTJ device (=bias voltage $\times$ (Rap-Rp)/Rap).

Fig. 8 shows the structure of the MTJ device and its operating principle.

Fig. 9 shows an example of the basic structure of an MRAM, Fig. 9(A) showing a perspective view of the MRAM, Fig. 9(B) showing a schematic circuit diagram, and Fig. 9(C) showing a cross-sectional view of an example of its structure.

Fig. 10 shows how the magnetoresistance of a conventional MTJ device using an amorphous Al-O as the tunnel barrier changes depending on the bias voltage.

Fig. 11 shows the structure of a MTJ device according to a variation of the invention, corresponding to Fig. 1(B).

## DESCRIPTION OF THE PREFERRED EMBODIMENTS

**[0012]** In the context of the present specification, because MgO has a cubic crystal structure (NaCl structure), the (001) plane, the (100) plane, and the (010) plane are all equivalent. The direction perpendicular to the film surface is herein considered to be the z-axis so that the film plane can be uniformly described as (001). Also in the context of the present specification, BCC structure, which is the crystalline structure of the ferromagnetic electrode layer, means body-centered cubic lattice structure. More specifically, BCC structure includes the BCC structure with no chemical ordering so-called A2-type structure, the BCC structure with chemical ordering such as B2-type structre and $L2_1$-type structure, and also the aforementioned structures with slight lattice distortion.

**[0013]** The term "ideal value" with regard to a perfect single-crystal without defect herein refers to a value that has been estimated from ultraviolet photoemission spectroscopy experiments (see W. Wulfhekel, et al.: Appl. Phys. Lett. 78 (2001) 509.). The term "ideal value" is used herein because the aforementioned state can be considered to be an upper limit value of the potential barrier height of the tunnel barrier of an ideal single-crystal MgO with hardly any oxygen vacancy defect or lattice defect.

**[0014]** Before describing the preferred embodiments of the invention, an analysis conducted by the inventors is discussed. The magnetoresistance (MR) ratio of a MTJ device can be expressed by the following equation:

$$\Delta R/Rp = (Rap - Rp)/Rp$$

where Rp and Rap indicate the tunnel junction resistance in the cases of parallel and antiparallel magnetization alignments, respectively, of two electrodes. According to the Jullire's formula, the MR ratio at low bias voltage can be expressed by:

$$\text{MR ratio} = (Rap - Rp)/Rp = 2P_1P_2/(1-P_1P_2), \text{ and}$$

$$P\alpha = (D\alpha \uparrow (E_F) - D\alpha \downarrow (E_F))/(D\alpha \uparrow (E_F) + D\alpha \downarrow (E_F),$$

$$\text{where } \alpha = 1, 2 \qquad (1)$$

**[0015]** In the above equations, $P\alpha$ is the spin polarization of an electrode, and $D\alpha \uparrow (E_F)$ and $D\alpha \downarrow (E_F)$ are the density of state (DOS) at the Fermi energy ($E_F$) of the majority-spin band and the minority-spin band, respectively. Since the spin polarization of ferromagnetic transition metals and alloys is approximately 0.5 or smaller, the Jullire's formula predicts a highest estimated MR ratio of about 70%.

**[0016]** Although the MR ratio of approximately 70% has been obtained at room temperature when a MTJ device was made using an amorphous Al-O tunnel barrier and polycrystalline electrodes, it has been difficult to obtain the output voltage of 200 mV, which is comparable to the output voltages of DRAMs, thereby preventing the realization of MRAM as mentioned above.

**[0017]** The inventors tried an approach to deposit a MTJ device in which the tunnel barrier comprises a single-crystal (001) of magnesium oxide (MgO) or a poly-crystalline MgO in which the (001) crystal plane is preferentially oriented. It is the inventors' theory that, because magnesium oxide is a crystal (where the atoms are arranged in an orderly fashion), as opposed to the conventional amorphous Al-O barrier, the electrons are not scattered and the coherent states of electrons are concerved during the tunneling process. Fig. 1(B) shows the MTJ device structure according to an embodiment of the invention. Fig. 1(A) shows the energy band structure of the ferromagnetic Fe(001), that is, the E-$E_F$ relationship with respect to the [001] direction of the momentum space. As shown in Fig. 1(B), the MTJ device structure of the present embodiment comprises a first Fe (001) layer 1, a second Fe (001) layer 5, and a poly-crystalline $MgO_x$ layer 3 with $0 < x < 1$ sandwiched therebetween, the polycrystalline layer having the (001) crystal plane preferentially oriented therein. According to the aforementioned Jullire's model, assuming that the momentum of the conduction electrons is preserved in the tunneling process, the tunneling current that passes through MgO would be dominated by those electrons with wave vector $k_z$ in the direction perpendicular to the tunnel barrier (normal to the junction interfaces). In accordance with the energy band diagram shown in Fig. 1(A) of Fe in the [001] ($\Gamma$-H) direction, the density of state (DOS) at the Fermi energy $E_F$ does not exhibit a very high spin polarization due to the fact that the sub-bands of the majority-spin and the minority-spin have states at the Fermi energy $E_F$. However, in case the coherent states of electrons are conserved in the tunneling process, only those conduction electrons that have totally symmetrical wave functions with respect to the axis perpendicular to the barrier would be coupled with the states in the barrier region and come to have a finite tunneling probability. The $\Delta 1$ band in the Fe(001) electrode has such totally symmetric wave functions. As shown in Fig. 1(A), the majority spin $\Delta 1$ band (solid line) has states at the Fermi energy $E_F$, whereas the minority spin $\Delta 1$ band (broken line) does not have state at the Fermi energy $E_F$. Because of such half-metallic characteristics of the Fe $\Delta_1$ band, there is the possibility that a very high MR ratio can be obtained in a coherent spin polarized tunneling. Since in an epitaxial (single-crystal, or (001) oriented poly-crystal) MTJ device the scattering of electrons is suppressed during the tunneling process, an epitaxial MTJ device is thought to be ideal for realizing the aforementioned coherent tunneling.

**[0018]** In the following, a MTJ device according to a first embodiment of the invention and a method of manufacturing the same will be described with reference to the drawings. Figs. 2(A) to 2(D) schematically show the method of manufacturing the MTJ device having the Fe (001)/MgO(001 )/Fe(001) structure according to the embodiment (to be hereafter referred to as a "Fe(001)/Mg0(001)/Fe(001) MTJ device"). Fe(001) refers to a ferromagnetic material with the BCC structure. First, a single-crystal MgO(001) substrate 11 was prepared. In order to improve the morphology of the surface of the single-crystal MgO(001) substrate 11, a MgO(001) seed layer 15 was grown by the molecular beam epitaxy (MBE) method. This was subsequently followed by the growth of an epitaxial Fe(001) lower electrode (first electrode) 17 with the thickness of 50 nm on the MgO(001) seed layer 15 at room temperature, as shown in Fig. 1(B), and then annealing was performed at 350°C under ultrahigh vacuum ($2 \times 10^{-8}$ Pa). Electron-beam evaporation conditions included an acceleration voltage of 8 kV, a growth rate of 0.02 nm/sec, and the growth temperature of room temperature (about

293K). The source material of the electron-beam evaporation was MgO of the stoichiometric composition (the ratio of Mg to O being 1:1), the distance between the source and the substrate was 40 cm, the base vacuum pressure was $1 \times 10^{-8}$ Pa, and the $O_2$ partial pressure was $1 \times 10^{-6}$ Pa. Alternatively, a source with oxygen vacancy defects may be used instead of the MgO of the stoichiometric composition (the ratio of Mg to O is 1:1).

**[0019]** Fig. 3(A) shows a RHEED image of the Fe(001) lower electrode (a first electrode). The image shows that the Fe(001) lower electrode (first electrode) 17 possesses a good crystallinity and flatness. Thereafter, a MgO(001) barrier layer 21 with the thickness of 2 nm was epitaxially grown on the Fe(001) lower electrode (first electrode) at room temperature, also using the MgO electron-beam evaporation method. Fig. 3(B) shows a RHEED image of the MgO(001) barrier layer 21. The image shows that the MgO(001) barrier layer 21 also possesses a good crystallinity and flatness.

**[0020]** As shown in Fig. 2(D), a Fe(001) upper electrode (a second electrode) 23 with the thickness of 10 nm was formed on the MgO(001) barrier layer 21 at room temperature. This was successively followed by the deposition of a Co layer 25 with the thickness of 10 nm on the Fe(001) upper electrode (second electrode) 23. The Co layer 25 is provided to increase the coercive force of the upper electrode 23 so as to realize the antiparallel magnetization alignment. The thus prepared sample was then processed by microfabrication techniques to obtain the Fe(001)/MgO(001)/Fe(001) MTJ device.

**[0021]** The aforementioned MgO evaporation using an electron beam involved the formation of a film under ultrahigh vacuum of $1.33 \times 10^{-7}$ ($10^{-9}$ Torr). It can be seen that in this method, the film, even when formed on a glass substrate to the thickness of 300 nm, was colorless and transparent, showing that a good crystal film was formed. Fig. 4 shows the results of observing the quadrupole mass spectra in the deposition chamber during the MgO growth. The results show that the partial pressures regarding the spectrum P1 of O and the spectrum P2 of $O_2$ are high. Fig. 5 shows the film deposition rate dependency of the oxygen partial pressure during MgO evaporation. It will be seen from the figure that the oxygen partial pressure itself is high, and that the oxygen partial pressure increases as the deposition rate increases. These results indicate the separation of oxygen from MgO during the deposition of MgO. Since the separated oxygen is pumped out of the deposition chamber using vacuum pumps, there is the possibility that there are oxygen vacancy defects such as $MgO_x$ ($0.9 < x < 1$). When there are oxygen vacancy defects, the potential barrier height of the MgO tunnel barrier is thought to decrease (such as in the range of 0.10 to 0.85 eV; more specifically, 0.2 to 0.5 eV), which is thought to result in an increase in the tunneling current. In the case of a typical Al-O tunnel barrier, the height of the tunnel barrier with respect to Fe(001) electrodes is considered to be 0.7 to 2.5 eV. An ideal tunnel barrier height of a MgO crystal is 3.6 eV, and experimental values of 0.9 to 3.7 eV have been obtained. Using the above-described method, a tunnel barrier height of approximately 0.3 eV is expected, indicating that the resistance of the tunnel barrier can be lowered. However, it should be noted that other factors, such as the influence of the aforementioned coherent tunneling, might also be involved. The value of x in $MgO_x$ due to oxygen vacancy defects is such that $0.98 < x < 1$, and more preferably $0.99 < x < 1$. These are the ranges such that the sole presence of Mg is excluded and the characteristics of MgO can be basically maintained.

**[0022]** The aforementioned tunnel barrier height $\phi$ was determined by fitting the electric conductance characteristics of the MTJ device (the relationship between tunnel current density J and bias voltage V) onto the Simmons' formula (Equation (20) in a non-patent document by J. G. Simmons: J. Appl. Phys. 34, pp. 1793-1803 (1963)) based on the WKB approximation, using the least squares method. The fitting was performed using the free electron mass ($m = 9.11 \times 10^{-31}$ kg) as the electron's effective mass. When a bias voltage V (which is normally on the order of 500 mV to 1000 mV) is applied until non-linearity appears in the J-V characteristics, the height $\phi$ of the tunnel barrier and the effective thickness $\Delta s$ of the tunnel barrier can be simultaneously determined by fitting the J-V characteristics using the Simmons' formula.

**[0023]** The effective thickness $\Delta s$ of the tunnel barrier was determined to be smaller than the thickness of the actual MgO(001) tunnel barrier layer ($t_{MgO}$) determined from a cross-sectional, transmission electron microscope image of the MTJ device by approximately 0.5 nm. This is the result of the effective thickness $\Delta s$ of the tunnel barrier having been reduced from the actual MgO(001) layer thickness by the effect of the image potential produced at the interface between the MgO(001) layer and the alloy layer consisting mainly of Fe and Co.

**[0024]** It is noted that, in the event that $t_{MgO}$ can be accurately determined using the cross-sectional transmission electron microscope (TEM) image, the height $\phi$ of the tunnel barrier can be more simply determined by the following technique. Namely, when the bias voltage V applied to the MTJ device is small (normally 100 mV or smaller), the tunnel current density J is proportional to the bias voltage V, such that the J-V characteristics become linear. In such a low-bias voltage region, the Simmons' formula can be described as follows:

$$J = [(2m\phi)^{1/2}/\Delta s](e/h)^2 \times \exp[-(4\pi\Delta s/h) \times (2m\phi)^{1/2}] \times V \qquad (2)$$

where m is the mass of the free electron ($9.11 \times 10^{-31}$ kg), e is the elementary electric charge ($1.60 \times 10^{-19}$C), and h

is the Planck's constant ($6.63 \times 10^{-34}$ J·s). The effective thickness of the tunnel barrier $\Delta s$ is approximately $t_{MgO}$ - 0.5 nm. By fitting the J-V characteristics of the MTJ device in the low-bias voltage region onto Equation (2), the height $\phi$ of the tunnel barrier can be simply and yet accurately estimated.

**[0025]** Fig. 6 shows a typical magnetoresistance curve of the Fe(001)/Mg0(001)/Fe(001) MTJ device produced by the above-described method. The MR ratio is 146% at the measurement temperature of 20K and 88% at the measurement temperature of 293K. These values represent the highest MR ratios that have so far been obtained at room temperature. Such high MR ratios cannot be explained by the spin polarization of the Fe(001) electrode and is thought rather to be related to a coherent spin-polarized tunneling. When 160 prototype MTJ devices were made, the variations regarding the MR ratio and tunneling resistance value were not more than 20%. The yield of the MTJ devices was 90% or more at the laboratory stage. These high values suggest the effectiveness of the approach of the invention. The resistance-area (RA) product of the MTJ device was on the order of a few $k\Omega\mu m^2$, which is suitable for MRAM.

**[0026]** Fig. 7(a) shows the bias voltage dependency of the MR ratio at room temperature. It will be seen that the bias voltage dependency of the MR ratio is fairly small. Although the characteristics are asymmetric, the voltage $V_{half}$ at which the MR ratio is reduced in half of the zero-bias value is 1250 mV, which is a very high value. In this connection, it is noted that the voltage $V_{half}$ at which the MR ratio is reduced in half of the zero-bias value in the conventional MTJs with Al-O tunnel barrier is 300 to 600 mV. Fig. 7(b) shows the output voltage $V_{out}$ of the MTJ device (=bias voltage $\times$ (Rap - Rp)/Rap). The maximum value of the output voltage $V_{out}$ is 380 mV with a positive bias. This value is about twice as large as that (a little less than 200 mV) in the case of the Al-O barrier. These high values in terms of both MR ratio and output voltage suggest the effectiveness of the technique according to the present embodiment.

**[0027]** Although in the above-described embodiment Fe(001) of BCC was employed, an Fe alloy of BCC, such as an Fe-Co alloy, Fe-Ni alloy, or Fe-Pt alloy, may be used instead. Alternatively, a layer of Co or Ni with the thickness of one or several monoatomic layers may be inserted between the electrode layer and the MgO(001) layer.

**[0028]** Hereafter, a MTJ device according to a second embodiment of the invention and a method of manufacturing the same will be described. In the method of manufacturing a Fe(001)/MgO(001)/Fe(001) MTJ device according to the present embodiment, MgO(001) is initially deposited in a poly-crystalline or amorphous state by sputtering or the like, and then an annealing process is performed such that a poly-crystal in which the (001) crystal plane is preferentially oriented is obtained. The sputtering conditions were such that, for example, the temperature was room temperature (293), a 5.08 cm (2-inch) $\phi$ MgO was used as a target, and sputtering was conducted in an Ar atmosphere. The acceleration power was 200 W and the growth rate was 0.008 nm/s. Because MgO that is deposited under these conditions is in an amorphous state, a crystallized MgO was obtained by increasing the temperature to 300°C from room temperature and maintaining that temperature for a certain duration of time.

**[0029]** Oxygen vacancy defects may be introduced by a method whereby oxygen vacancy defects is produced during growth, a method whereby oxygen vacancy defects is introduced subsequently, or a method whereby a state with oxygen vacancy defects is subjected to an oxygen plasma process or natural oxidation so as to achieve a certain oxygen deficit level.

**[0030]** As described above, in accordance with the MTJ device technology of the present embodiment, an annealing process is carried out for crystallization after an amorphous MgO has been deposited by sputtering, thereby eliminating the need for large-sized equipment.

**[0031]** Hereafter, a MTJ device according to a variation of the above-described embodiments will be described with reference to the drawings. Fig. 11 shows the structure of the MTJ device according to the variation, which corresponds to Fig. 1(B). As shown in Fig. 11, the MTJ device of the variation is characterized in that, as in the MTJ device of the above-described embodiments, the electrodes disposed on either side of a single-crystal $MgO_x$(001) layer 503 or an oxygen-deficit poly-crystal $MgO_x$ ($0 < x < 1$) in which the (001) crystal plane is preferentially oriented comprises an amorphous ferromagnetic alloy, such as CoFeB layers 501 and 505. The amorphous ferromagnetic alloy can be formed by evaporation or sputtering, for example. The resultant characteristics are substantially identical to those of the first embodiment.

**[0032]** As the amorphous magnetic alloy, FeCoB; FeCoBSi, FeCoB-P, FeZr, and CoZr may be used, for example. Although an anneal process after the preparation of the MTJ device might cause the amorphous magnetic alloy in the electrode layers to be partially or entirely crystallized, this would not lead to a significant deterioration of the MR ratio. Thus, such a crystallized amorphous magnetic alloy may be used in the electrode layers.

**[0033]** While the MTJ device according to various embodiments of the invention has been described, it should be apparent to those skilled in the art that the invention is not limited to those specific embodiments and various other modifications, improvements and combinations are possible. For example, the height of the tunnel barrier may be adjusted by doping Ca or Sr, instead of introducing an oxygen vacancy defects to the MgO layer. Further, while the MgO layer has been described to be deposited by electron-beam evaporation or sputtering, it should be obvious that other deposition methods are also possible. The term "high vacuum" refers to values on the order of no more than $10^{-6}$ Pa in the case where oxygen is not introduced, for example. In the case where oxygen is introduced, the term refers to values on the order of $10^{-4}$ Pa.

**[0034]** In accordance with the invention, a larger magnetoresistance than in the conventional MTJ device can be obtained, and the output voltage of the MTJ device can be increased. At the same time, the resistance value of the MTJ device can be reduced so that it is optimized for MRAM. The invention thus enables the level of integration of MRAM using the MTJ device to be readily increased. In accordance with the invention, the output voltage value of the MRAM roughly doubles over prior art, making the MTJ device of the invention suitable for very large scale integrated MRAMs of gigabit class.

## Claims

1. A magnetoresistive device comprising a magnetic tunnel junction structure comprising:

   a tunnel barrier layer;
   a first ferromagnetic material layer of an Fe alloy with the BCC structure formed on a first side of said tunnel barrier layer; and
   a second ferromagnetic material layer of an Fe alloy with the BCC structure formed on a second side of said tunnel barrier layer, **characterised in that**
   said tunnel barrier layer is formed by a poly-crystalline $MgO_x$, wherein x is $0<x<1$, in which the (001) crystal plane is preferentially oriented, and
   a potential barrier height of said tunnel barrier between the bottom of the conduction band of said tunnel barrier layer and the Fermi energy of at least one of said first and said second ferromagnetic layers is in the range of 0.2 to 0.5 eV.

2. The magnetoresistive device of claim 1, wherein
   said Fe alloy is FeCoB alloy.

3. A tunnel barrier layer deposited on a ferromagnetic material layer of an Fe alloy with the BCC structure, wherein
   said tunnel barrier layer is formed by a polycrystalline $MgO_x$, wherein x is $0<x<1$, in which the (001) crystal plane is preferentially oriented, and
   the potential barrier height of said tunnel barrier is in the range of 0.2 to 0.5 eV.

4. A method of manufacturing a magnetoresistive device comprising:

   preparing a substrate;
   depositing a first amorphous ferromagnetic material layer comprising an amorphous Fe alloy on said substrate;
   forming an amorphous magnesium oxide layer on said first ferromagnetic material layer and then crystallizing said amorphous magnesium oxide layer by annealing so as to form a tunnel barrier layer comprising a poly-crystalline magnesium oxide in which the (001) crystal plane is preferentially oriented; and
   depositing a second amorphous ferromagnetic material layer comprising an amorphous Fe alloy on said tunnel barrier layer.

5. The method of manufacturing a magnetoresistive device according to claim 4, wherein
   said poly-crystalline magnesium oxide has oxygen vacancy defects.

6. The method of manufacturing a magnetoresistive device according to claim 4, wherein
   the potential barrier height of said tunnel barrier is in the range of 0.2 to 0.5 eV.

7. The method of manufacturing a magnetoresistive device according to claim 4, wherein
   said Fe alloy is FeCoB alloy.

8. The method of manufacturing a magnetoresistive device according to claim 4, further comprising the step of:

   annealing the device so as to partially or entirely crystallize said amorphous ferromagnetic material.

## Patentansprüche

1. Magnetwiderstandsvorrichtung, aufweisend eine magnetische Tunnelkontaktstruktur, die Folgendes aufweist:

eine Tunnelbarriereschicht;
eine erste Schicht aus ferromagnetischem Material aus einer Fe-Legierung mit BCC-Struktur (= kubisch innenzentrierte Struktur), die auf einer ersten Seite der besagten Tunnelbarriereschicht ausgebildet ist; und
eine zweite Schicht aus ferromagnetischem Material aus einer Fe-Legierung mit BCC-Struktur, die auf einer zweiten Seite der besagten Tunnelbarriereschicht ausgebildet ist,
**dadurch gekennzeichnet, dass**
die besagte Tunnelbarriereschicht durch ein polykristallines $MgO_x$ ausgebildet ist, wobei x gleich $0<x<1$ ist, in dem die (001) Kristallebene vorzugsweise ausgerichtet ist, und
eine potenzielle Barrierehöhe der besagten Tunnelbarriere zwischen dem Boden des Leitungsbandes der besagten Tunnelbarriereschicht und der Fermi-Energie von zumindest einer der besagten ersten und der besagten zweiten ferromagnetischen Schicht im Bereich von 0,2 bis 0,5 eV liegt.

**2.** Magnetwiderstandsvorrichtung nach Anspruch 1, wobei die besagte Fe-Legierung eine FeCoB-Legierung ist.

**3.** Tunnelbarriereschicht, die auf einer Schicht aus ferromagnetischem Material aus einer Fe-Legierung mit BCC-Struktur abgeschieden ist, wobei
die besagte Tunnelbarriereschicht aus polykristallinem $MgO_x$ ausgebildet ist, wobei x gleich $0<x<1$ ist, in dem die (001) Kristallebene vorzugsweise ausgerichtet ist, und
die potentielle Barrierehöhe der besagten Tunnelbarriere im Bereich von 0,2 bis 0,5 eV liegt.

**4.** Verfahren zur Herstellung einer Magnetwiderstandsvorrichtung, aufweisend:

Herstellung eines Substrats;
Abscheidung einer ersten Schicht aus amorphem ferromagnetischen Material, die eine amorphe Fe-Legierung aufweist, auf dem besagten Substrat;
Ausbildung einer Schicht aus amorphem Magnesiumoxid auf der besagten ersten Schicht aus ferromagnetischem Material und dann Kristallisierung der besagten Schicht aus amorphem Magnesiumoxid durch Glühen, so dass eine Tunnelbarriereschicht ausgebildet wird, die ein polykristallines Magnesiumoxid aufweist, in dem die (001) Kristallebene vorzugsweise orientiert ist; und
Abscheidung einer zweiten Schicht aus amorphem ferromagnetischen Material, die eine amorphe Fe-Legierung aufweist, auf der besagten Tunnelbarriereschicht.

**5.** Verfahren zur Herstellung einer Magnetwiderstandsvorrichtung nach Anspruch 4, wobei
das besagte polykristalline Magnesiumoxid Sauerstoffleerstellendefekte aufweist.

**6.** Verfahren zur Herstellung einer Magnetwiderstandsvorrichtung nach Anspruch 4, wobei
die potentielle Barrierehöhe der besagten Tunnelbarriere im Bereich von 0,2 bis 0,5 eV liegt.

**7.** Verfahren zur Herstellung einer Magnetwiderstandsvorrichtung nach Anspruch 4, wobei
die besagte Fe-Legierung eine FeCoB-Legierung ist.

**8.** Verfahren zur Herstellung einer Magnetwiderstandsvorrichtung nach Anspruch 4, weiterhin aufweisend den folgenden Schritt:

Glühen der Vorrichtung, so dass das besagte amorphe ferromagnetische Material teilweise oder ganz kristallisiert wird.

**Revendications**

**1.** Un dispositif magnétorésistif comportant une structure de jonction à effet tunnel magnétique, comprenant :

une couche-barrière à effet tunnel ;
une première couche de matériau ferromagnétique en un alliage de Fe avec la structure de BCC formée d'un premier côté de ladite couche-barrière à effet tunnel ; et
une deuxième couche de matériau ferromagnétique en un alliage de Fe avec la structure de BCC formée d'un second coté de ladite couche-barrière à effet tunnel, **caractérisée en ce que**
ladite couche-barrière à effet tunnel est constituée par un $MgO_x$ polycristallin, où x est tel que $0<x<1$, le plan

cristallin (001) est préférentiellement orienté, et
une hauteur de barrière potentielle de ladite barrière à effet tunnel, entre le fond de la bande de conduction de ladite couche-barrière à effet tunnel et l'énergie de Fermi d'au moins une parmi lesdites première et seconde couches ferromagnétiques est située dans la plage allant de 0,2 à 0,5 eV.

**2.** Le dispositif magnétorésistif selon la revendication 1, dans lequel ledit alliage de Fe est un alliage de FeCoB.

**3.** Une couche-barrière à effet tunnel déposée sur une couche de matériau ferromagnétique en un alliage de Fe avec la structure de BCC, dans lequel
ladite couche-barrière à effet tunnel est constituée par un $MgO_x$ polycristallin, où x est tel que $0<x<1$, dans lequel le plan cristallin (001) est préférentiellement orienté, et
la hauteur de la barrière potentielle de ladite barrière à effet tunnel est située dans la plage allant de 0,2 à 0,5 eV.

**4.** Une méthode pour fabriquer un dispositif magnétorésistif comprenant :

la préparation d'un substrat ;
le dépôt d'une première couche amorphe de matériau ferromagnétique comportant un alliage amorphe de Fe sur ledit substrat ;
la formation d'une couche amorphe d'oxyde de magnésium sur ladite première couche de matériau ferromagnétique et puis la cristallisation de ladite couche amorphe d'oxyde de magnésium par recuit de manière à former une couche-barrière à effet tunnel comportant un oxyde de magnésium polycristallin dans laquelle le plan cristallin (001) est préférentiellement orienté ; et
le dépôt d'une deuxième couche amorphe de matériau ferromagnétique comportant un alliage amorphe de Fe sur ladite couche-barrière à effet tunnel.

**5.** La méthode pour fabriquer un dispositif magnétorésistif selon la revendication 4, dans laquelle
ledit oxyde de magnésium polycristallin a des défauts de type lacune d'oxygène.

**6.** La méthode pour fabriquer un dispositif magnétorésistif selon la revendication 4, dans laquelle
la hauteur de barrière potentielle de ladite barrière à effet tunnel est située dans la plage allant de 0,2 à 0,5 eV.

**7.** La méthode pour fabriquer un dispositif magnétorésistif selon la revendication 4, dans laquelle
ledit alliage de Fe est un alliage de FeCoB.

**8.** La méthode pour fabriquer un dispositif magnétorésistif selon la revendication 4, comportant en outre l'étape de :

recuit du dispositif de manière à partiellement ou entièrement cristalliser ledit matériau ferromagnétique amorphe.

FIG. 1 (A)

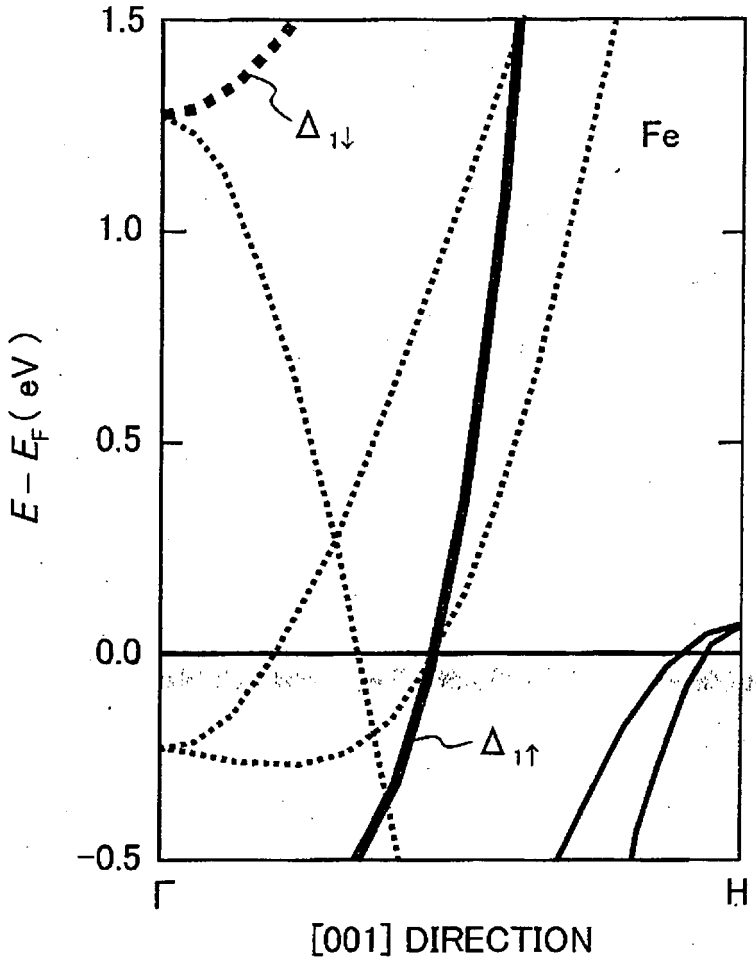
1.5
1.0
0.5
0.0
−0.5
E − E_F ( eV )
Δ1↓
Fe
Δ1↑
Γ
H
[001] DIRECTION

FIG. 1 (B)

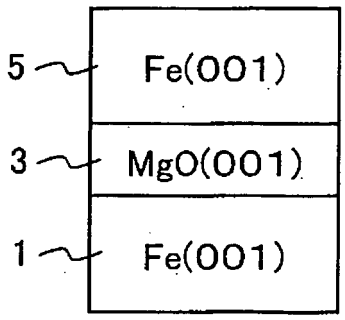
5
Fe(001)
3
MgO(001)
1
Fe(001)

FIG. 2 (A)

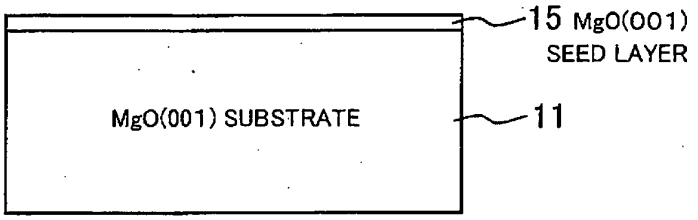


FIG. 2 (B)

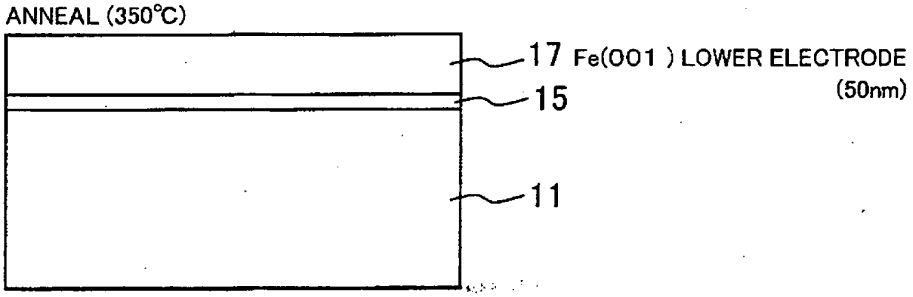


FIG. 2 (C)

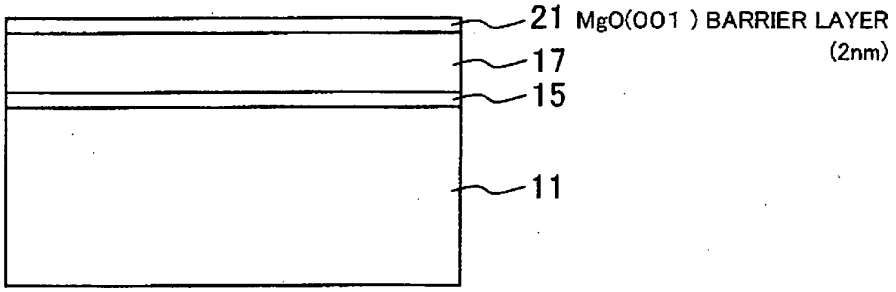


FIG. 2 (D)

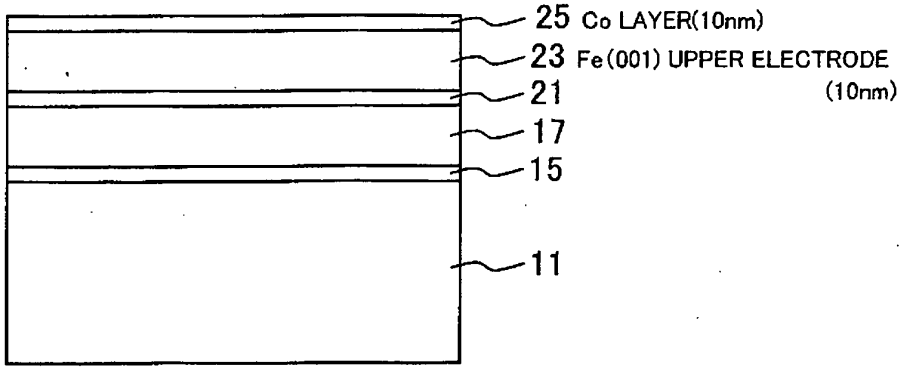

FIG. 3 (A)

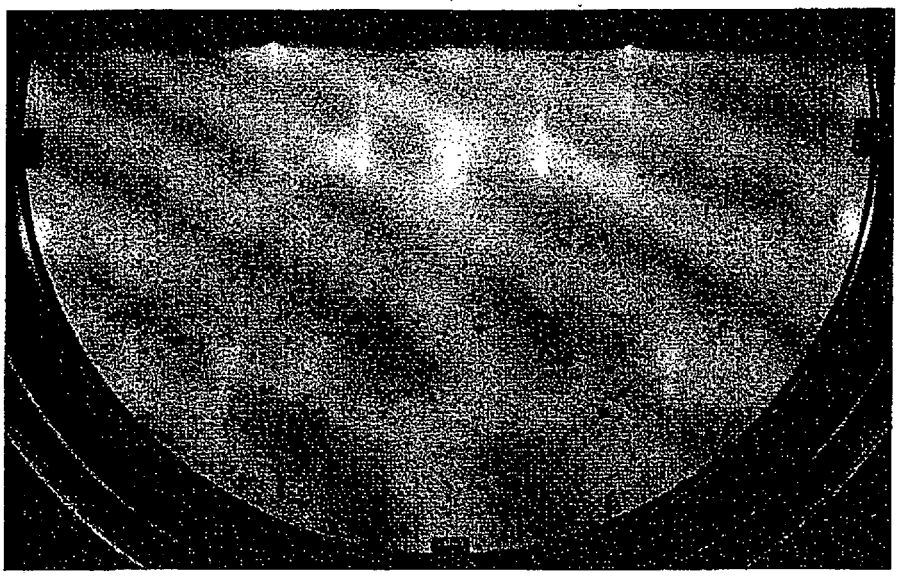

FIG. 3 (B)

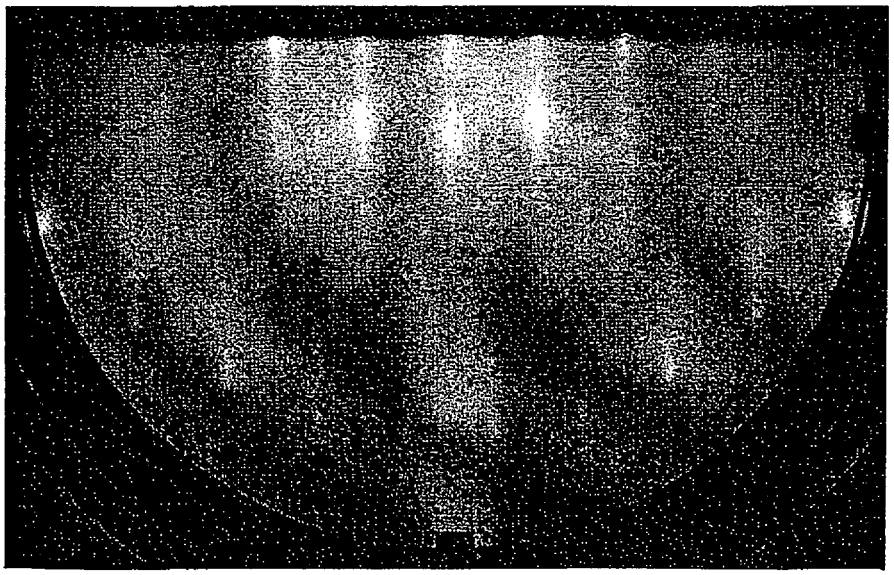

FIG. 4

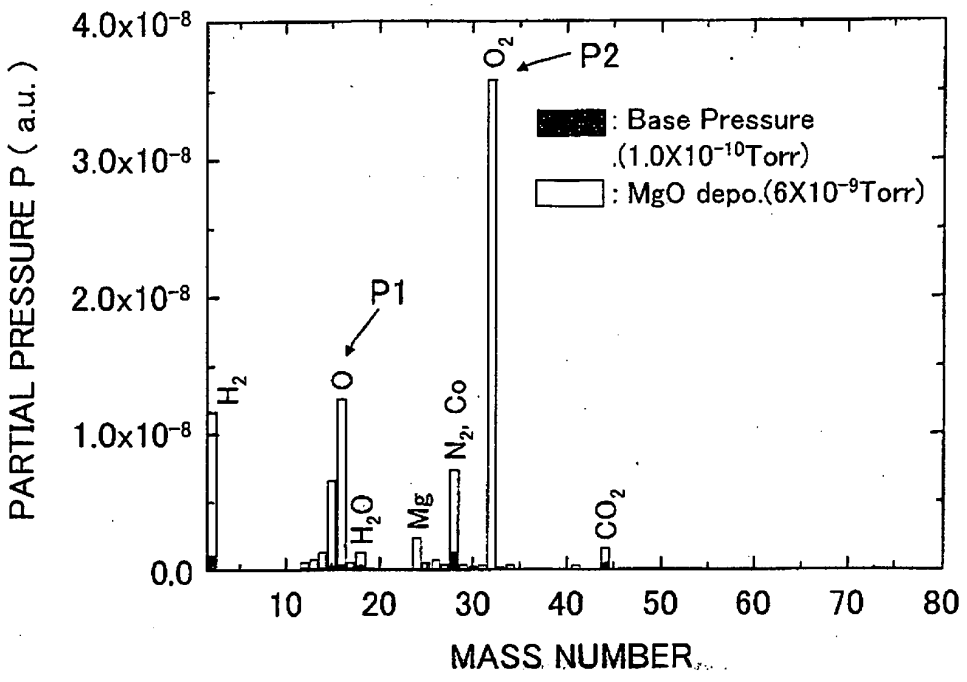


MASS SPECTRA

FIG. 5

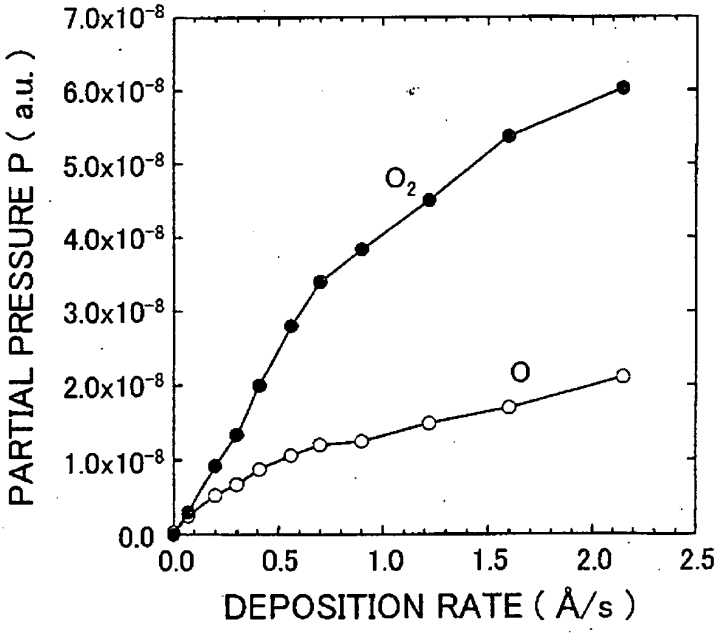


OXYGEN PARTIAL PRESSURE DURING MgO EVAPORATION

FIG. 6

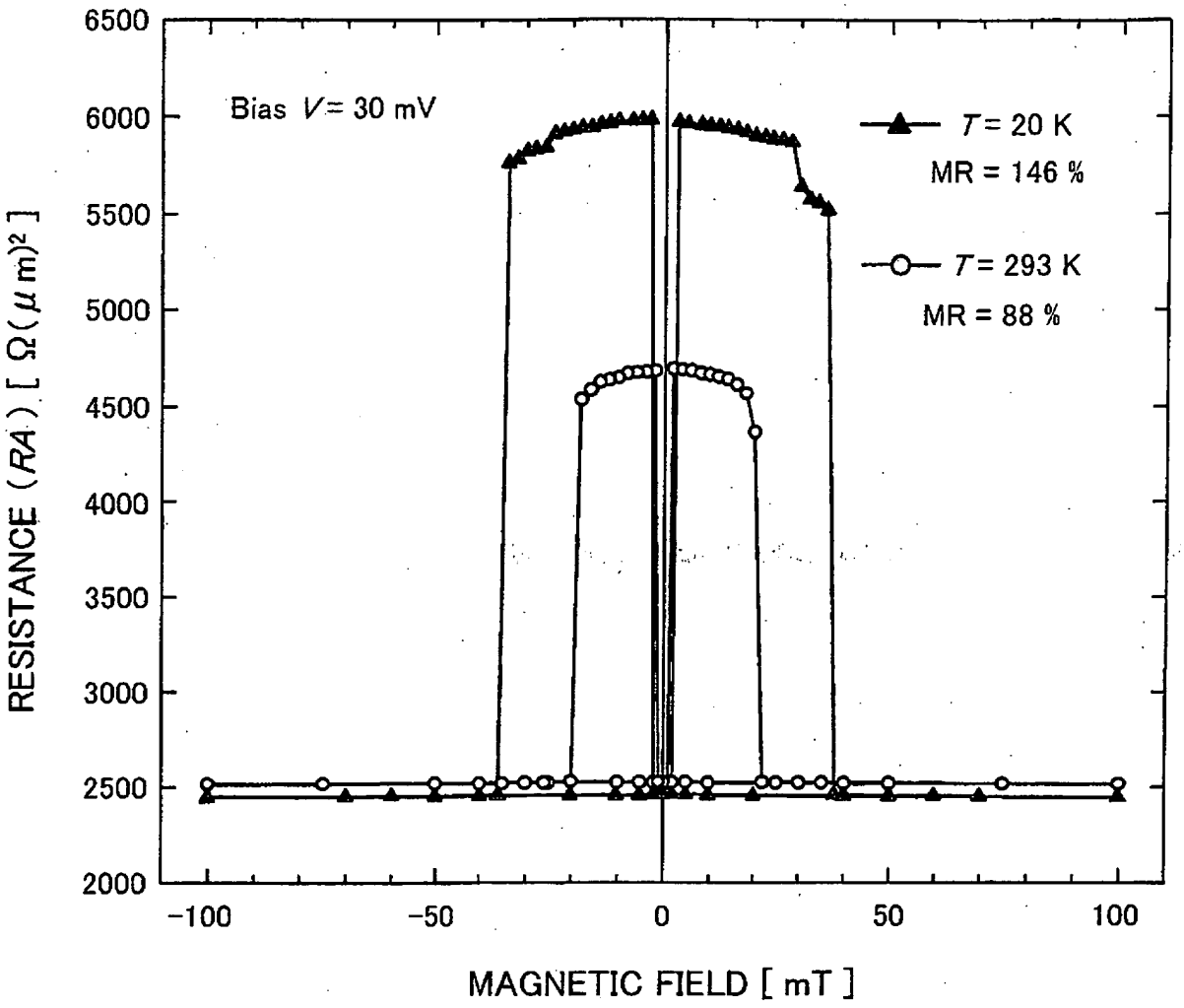
Bias V = 30 mV
T = 20 K
MR = 146 %
T = 293 K
MR = 88 %
RESISTANCE (RA) [ Ω(μm)² ]
MAGNETIC FIELD [ mT ]
6500
6000
5500
5000
4500
4000
3500
3000
2500
2000
−100
−50
0
50
100

FIG. 7 (A)

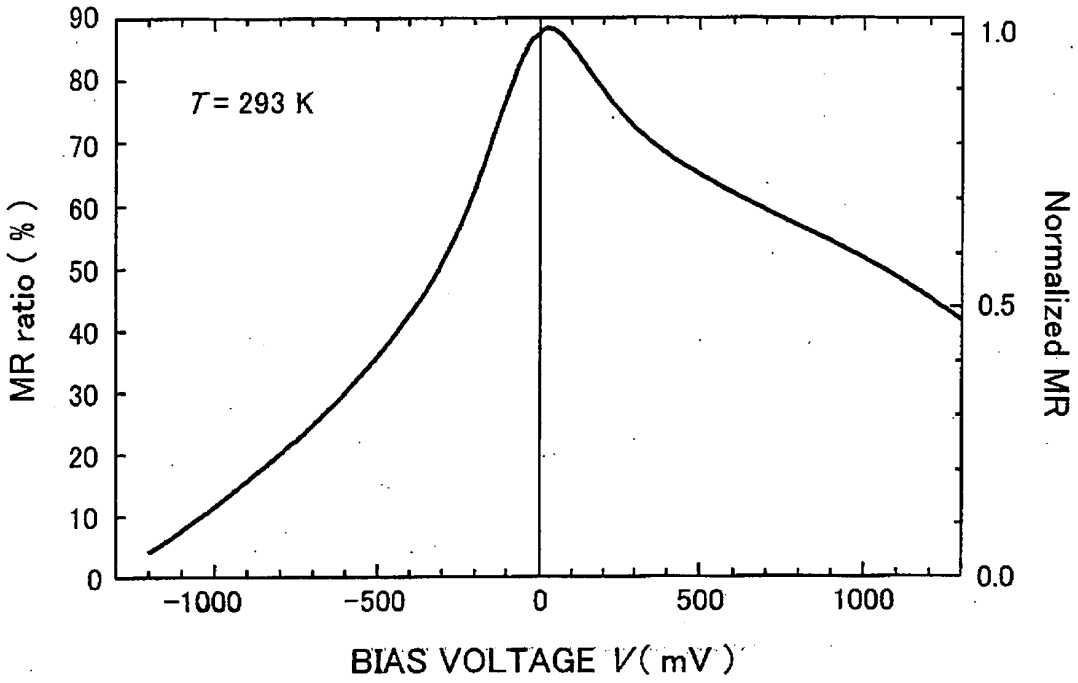
T = 293 K
MR ratio ( % )
Normalized MR
BIAS VOLTAGE V ( mV )
90
80
70
60
50
40
30
20
10
0
1.0
0.5
0.0
-1000
-500
0
500
1000

FIG. 7 (B)

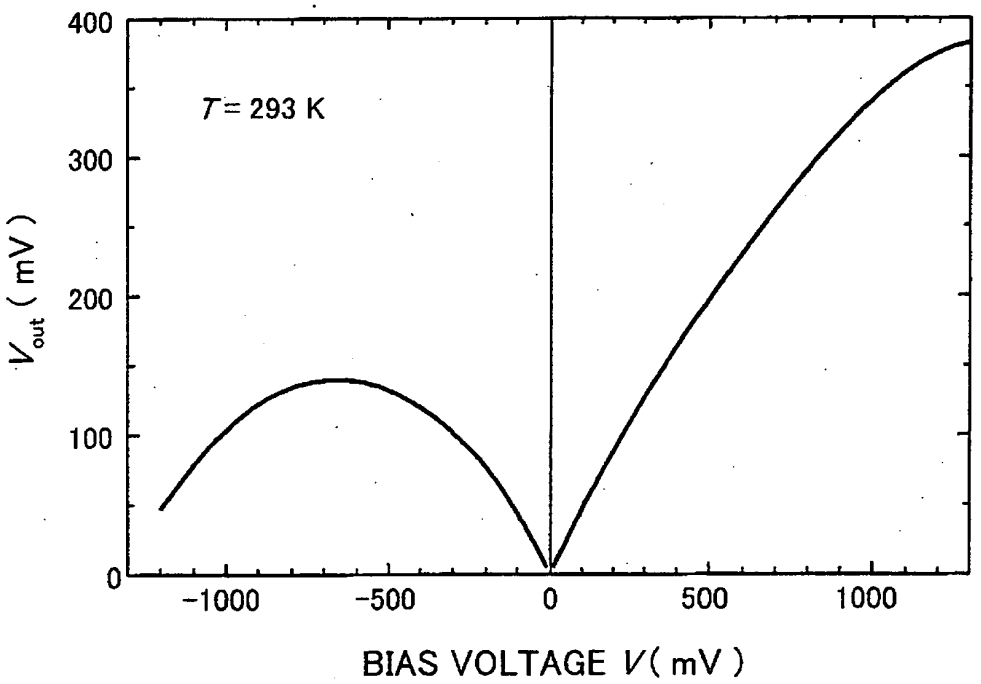
T = 293 K
$V_{out}$ ( mV )
BIAS VOLTAGE V ( mV )
400
300
200
100
0
-1000
-500
0
500
1000

FIG. 8 (A)

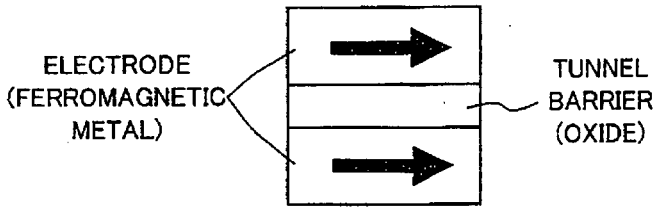


FIG. 8 (B)

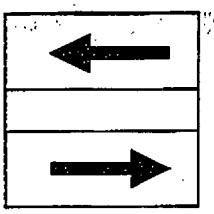

FIG. 9 (A)

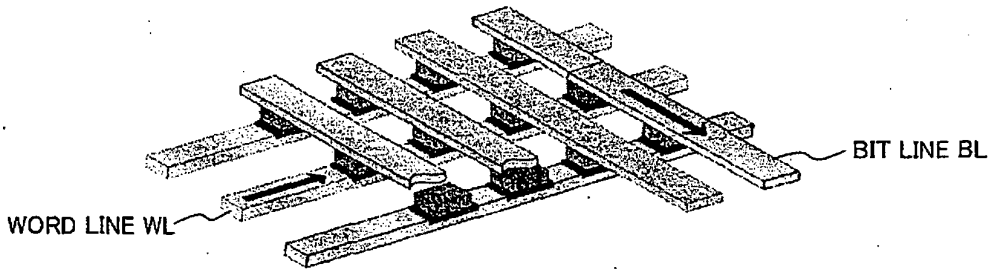


FIG. 9 (B)

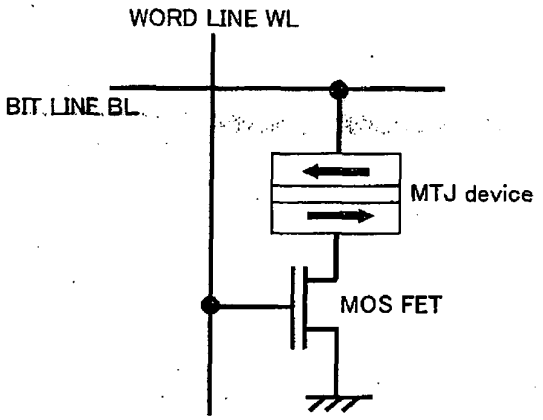


FIG. 9 (C)

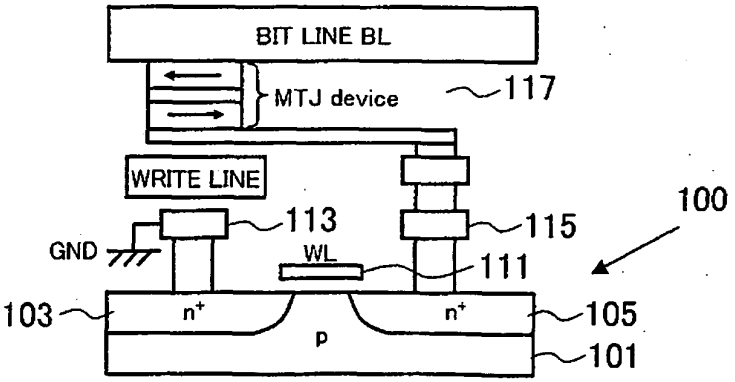


MOSFET 100

FIG. 10

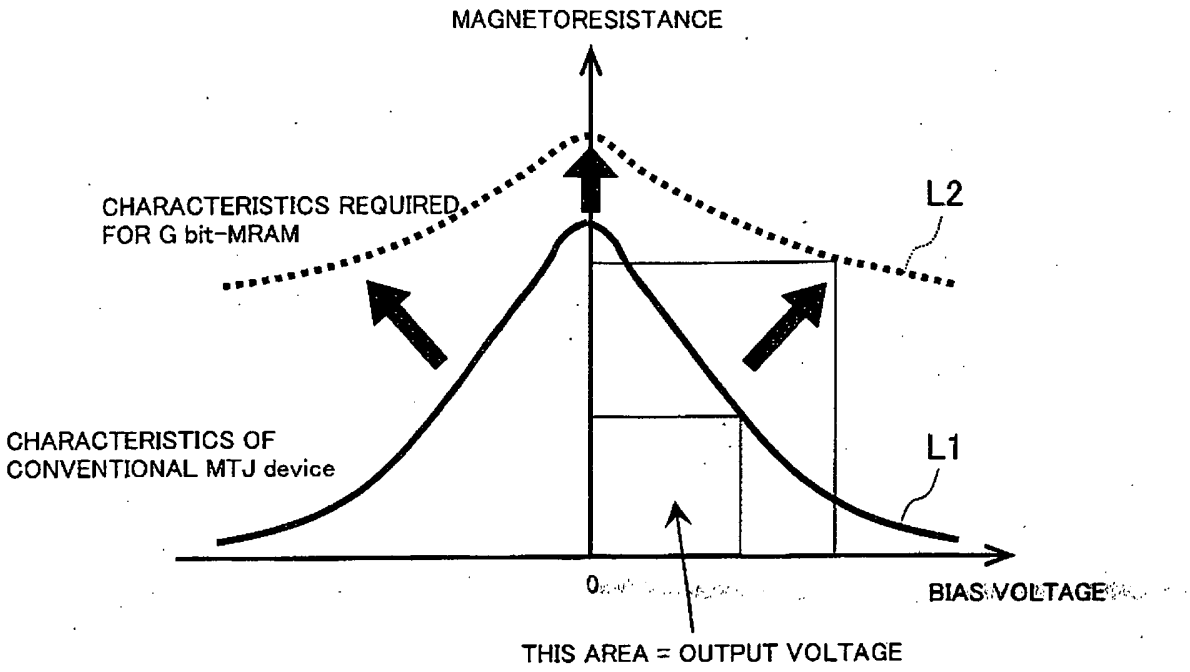
MAGNETORESISTANCE
CHARACTERISTICS REQUIRED FOR G bit-MRAM
L2
CHARACTERISTICS OF CONVENTIONAL MTJ device
L1
0
BIAS VOLTAGE
THIS AREA = OUTPUT VOLTAGE

FIG. 11

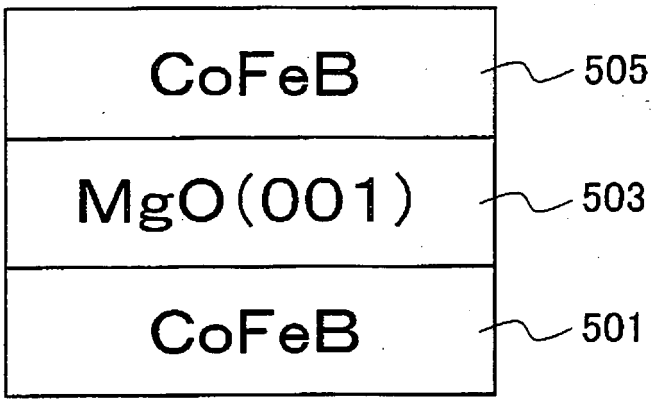

## REFERENCES CITED IN THE DESCRIPTION

*This list of references cited by the applicant is for the reader's convenience only. It does not form part of the European patent document. Even though great care has been taken in compiling the references, errors or omissions cannot be excluded and the EPO disclaims all liability in this regard.*

### Non-patent literature cited in the description


- **D. Wang et al.** *Science,* 2001, vol. 294, 1488 **[0005]**
- **S. Mitani et al.** *Journal of Applied Physics,* 2003, vol. 93, 8041-8043 **[0005]**
- **J. G. Simmons.** *J. Appl. Phys.,* 1963, vol. 34, 1793-1803 **[0022]**